



## Spectacular Effects of Ultraviolet C Radiation, Gamma Radiation, X-Ray Radiation & Heat Treatment on Disinfection Rate of SARS- COVID Virus-2

Dr. Gayaan Singh<sup>1</sup> Dr. Vinay Dua<sup>2</sup>

Assistant Professor, Department Of Physics, G.M.V.College, Rampur Maniharan Saharanpur UP,INDIA

Assistant Professor & Head, Department Of Physics, R.S.M. College, Dhampur (Bijnor) UP,INDIA

### ABSTRACT

Severe acute respiratory syndrome (SARS) is a newly emerging infectious disease caused by a novel coronavirus, SARS-coronavirus (SARS-CoV). The SARS-CoV spike (S) protein is composed of two subunits; the S1 subunit contains a receptor-binding domain that engages with the host cell receptor angiotensin-converting enzyme 2 and the S2 subunit mediates fusion between the viral and host cell membranes. The S protein plays key parts in the induction of neutralizing-antibody and T-cell responses, as well as protective immunity, during infection with SARS-CoV. In this Review, we highlight recent advances in the development of vaccines<sup>1</sup> and therapeutics based on the S protein. A direct approach to limit airborne viral transmissions is to inactivate them within a short time of their production. Germicidal ultraviolet light, typically at 254nm, is effective in this context but, used directly, can be a health hazard to skin and eyes. By contrast, far-UVC light (207–222nm) efficiently kills pathogens potentially without harm to exposed human tissues. It is previously demonstrated that 222-nm far-UVC light efficiently kills airborne influenza virus and we extend those studies to explore far-UVC efficacy against airborne human coronaviruses alpha HCoV-229E and beta HCoV-OC43. Low doses of 1.7 and 1.2 mJ/cm<sup>2</sup> inactivated 99.9% of aerosolized coronavirus 229E and OC43, respectively. As all human coronaviruses have similar genomic sizes, far-UVC light would be expected to show similar inactivation efficiency against other human coronaviruses including SARS-CoV-2. Based on the beta-HCoV-OC43 results, continuous far-UVC exposure in occupied public locations at the current regulatory exposure limit (~3 mJ/cm<sup>2</sup>/hour) would result in ~90% viral inactivation in ~8minutes, 95% in ~11minutes, 99% in ~16minutes and 99.9% inactivation in ~25minutes. Thus while staying within current regulatory dose limits, low-dose-rate far-UVC exposure can potentially safely provide a major reduction in the ambient level of airborne coronaviruses in occupied public locations. With nearly every country combating the 2019 novel coronavirus (COVID-19), there is a need to understand how local environmental conditions may modify transmission. To date, quantifying seasonality of the disease has been limited by scarce data and the difficulty of isolating climatological variables from other drivers of transmission in observational studies. We combine a spatially resolved dataset of confirmed COVID-19 cases, composed of 3,235 regions across 173 countries, with local environmental conditions and a statistical approach developed to quantify causal effects of environmental conditions in observational data settings. We find that ultraviolet (UV) radiation has a statistically significant effect on daily COVID-19 growth rates: a SD increase in UV lowers the daily growth rate of COVID-19 cases by 1 % point over the subsequent 2.5 weeks, relative to an average in-sample growth rate of 13.2%. The time pattern of lagged effects peaks 9 to 11 d after UV exposure, consistent with the combined timescale of incubation, testing, and reporting. Cumulative effects of temperature and humidity are not statistically significant. Simulations illustrate how seasonal changes in UV have influenced regional patterns of COVID-19 growth rates from January to June, indicating that UV has a substantially smaller effect on the spread of the disease than social distancing policies. Furthermore, total COVID-19 seasonality has indeterminate sign for most regions during this period due to uncertain effects of other environmental variables. Our findings indicate UV exposure influences COVID-19 cases, but a comprehensive understanding of seasonality awaits further analysis.

**Keywords:** SARS-CoV-2, UV radiation,  $\gamma$  radiation, radiation attenuation X-Ray radiation protein spikes.

### INTRODUCTION

In late previous year, an outbreak of unusual life-threatening respiratory disease of unknown aetiology began in Guangdong Province, China. This disease was designated severe acute respiratory syndrome (SARS) and was later determined to be caused by a novel coronavirus, termed SARS-CoV. Since the identification of coronavirus as the infectious agent for SARS, numerous laboratories have begun research on this virus. According to the WHO, 8098 people were diagnosed with SARS and 774 people died of this disease during the initial outbreak of 2003. Due to the severity of SARS disease and the contagious nature of the causal agent, the WHO has provided guidelines for working safely with this coronavirus. The WHO recommends biosafety level 3 (BSL3) as the appropriate containment level for working with live SARS-CoV, and there is a concern that another SARS outbreak could occur following an accidental exposure in a laboratory. Since the end of the SARS epidemic in July 2003, there have been three

known cases of SARS in laboratory researchers due to accidental exposure to the virus. Successful inactivation of the virus allows the transfer of material from a BSL3 to a BSL2 environment and may reduce the risk of accidental infections through unsafe laboratory practices. Inactivated cell-culture derived viral stocks may also be useful for the development of vaccines and the study of their safety and immunogenicity<sup>2</sup>. We examined the efficiency of several methods of viral inactivation, including methods that may inhibit viral replication or entry.

## MATERIALS & METHODS

### VIRUS AND CELLS

Initially infected African green monkey kidney (Vero E6) cells with SARS-CoV (Urbani strain) that was kindly provided by Drs. L.J. Anderson and T.G. Ksiazek from the Centers for Disease Control and Prevention, Atlanta, GA. Briefly, Vero E6 monolayer cells were infected by inoculating cultures with 50  $\mu$ l of virus ( $10^{6.33}$  TCID<sub>50</sub> per ml) in a

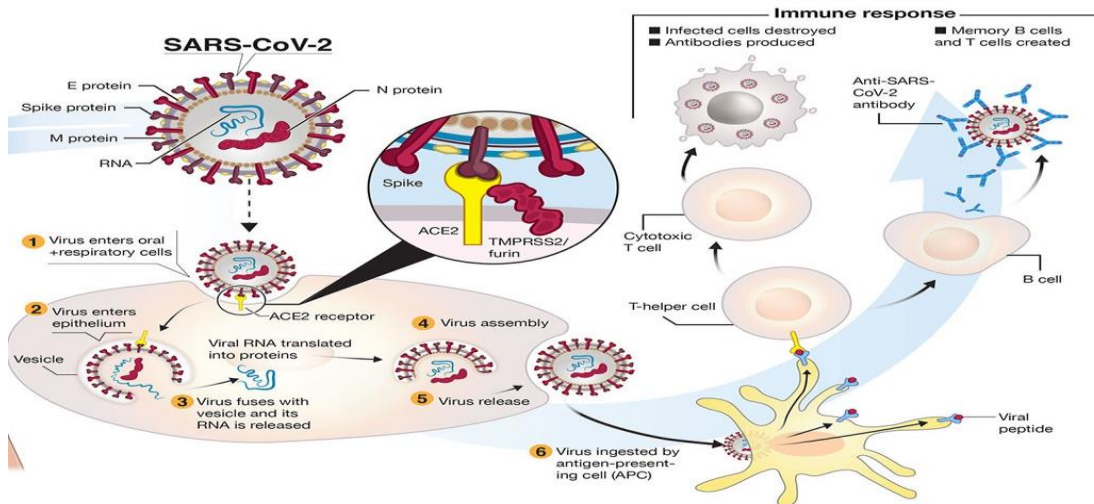


**Fig 1: Infected Cells Destruction, Antibodies Production & Creation of Memory B Cells & T Cells**

Final volume of 5 ml Dulbecco's modified Eagle's medium (DMEM) (Biosource International, Camarillo, CA) in T150 flasks for 1 h at 25 °C. Dulbecco's modified Eagle's medium containing supplements (10% fetal bovine serum, 2 mM/ml L-glutamine, 100 U/ml penicillin, 100  $\mu$ g/ml streptomycin, and 0.5  $\mu$ g/ml fungizone) (Biosource International) was added to the flask and the cells were incubated at 37 °C for 3 days. Supernatant was collected, clarified by centrifugation, and stored at -70 °C as the viral stock [Fig 1]. The Vero cells were maintained in DMEM with supplements<sup>3</sup>. All personnel wore powered air-purifying respirators (3 M, Saint Paul, MN) and worked with infectious virus inside a biosafety cabinet, within a BSL3 containment facility.

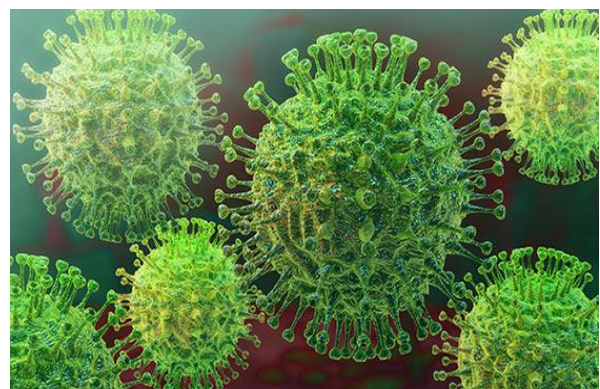
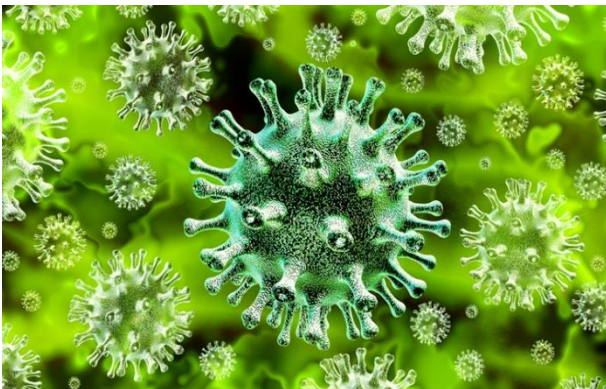


**Fig2: Structure of Virus**

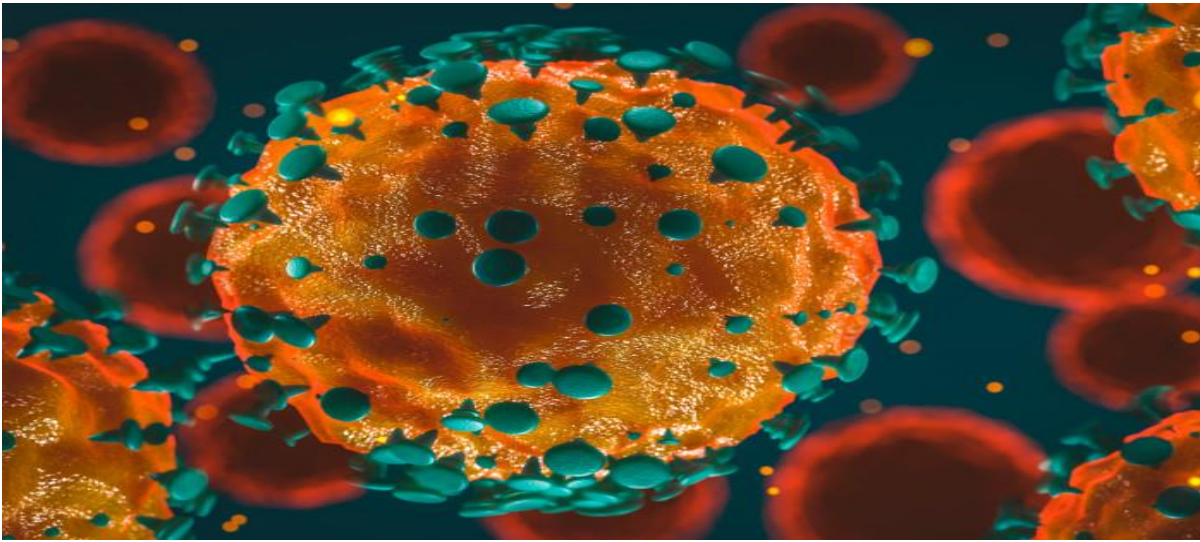


**Fig3: Corona Virus with Greater Risk of Black Fungus**

### **QUANTITATION OF VIRAL TITERS**

Viral titers were determined in Vero cell monolayers on 24 and 96-well plates using a 50% tissue culture infectious dose assay (TCID<sub>50</sub>). Serial dilutions of virus samples were incubated at 37 °C for 4 days and subsequently examined for cytopathic effect (CPE) in infected cells, as described by Ksiazek . Briefly, SARS-CoV-induced CPE of infected cells was determined by observing rounded, detached cells in close association to each other. Evidence of inactivation was determined by absence of CPE in Vero cells, indicating loss of infectivity.

### **UV LIGHT TREATMENT**

Ultraviolet light (UV) treatment was performed on 2 ml aliquots of virus (volume depth = 1 cm) in 24-well plates (Corning Inc., Corning, NY). The UV light source (Spectronics Corporation, Westbury, NY)<sup>4</sup> was placed above the plate, at a distance of 3 cm from the bottom of the wells containing the virus samples [Fig4]. At 3 cm our UVC light source (254 nm) emitted 4016  $\mu\text{W}/\text{cm}^2$  (where  $\mu\text{W} = 10^{-6} \text{ J/s}$ ) and the UVA light source (365 nm) emitted 2133  $\mu\text{W}/\text{cm}^2$ , as measured by radiometric analysis (Spectronics Corporation). After exposure to the UV light source, virus was frozen for later analysis by TCID<sub>50</sub> assay using CPE as the endpoint [Fig 5].

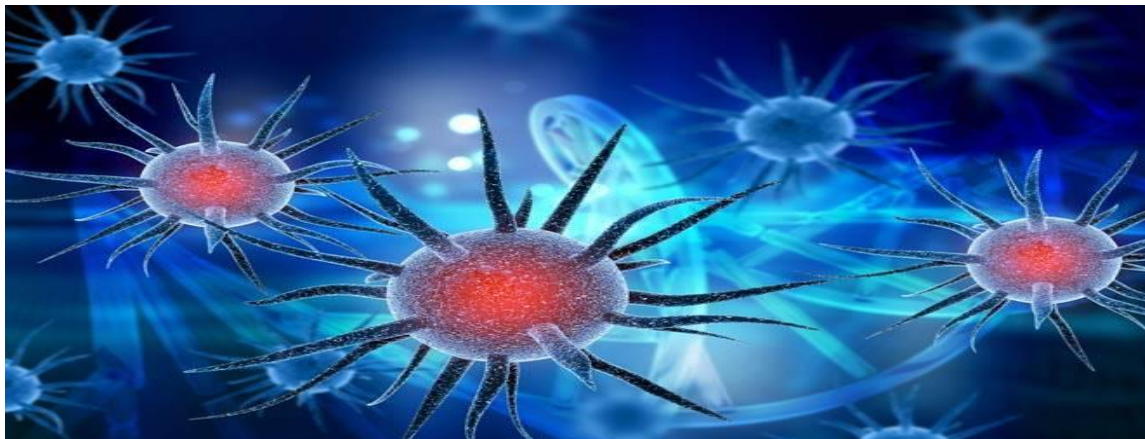


**Fig4: Technology to kill coronavirus with UV light in ten minutes**



**Fig 5: Effect of UV Treatment on DNA**

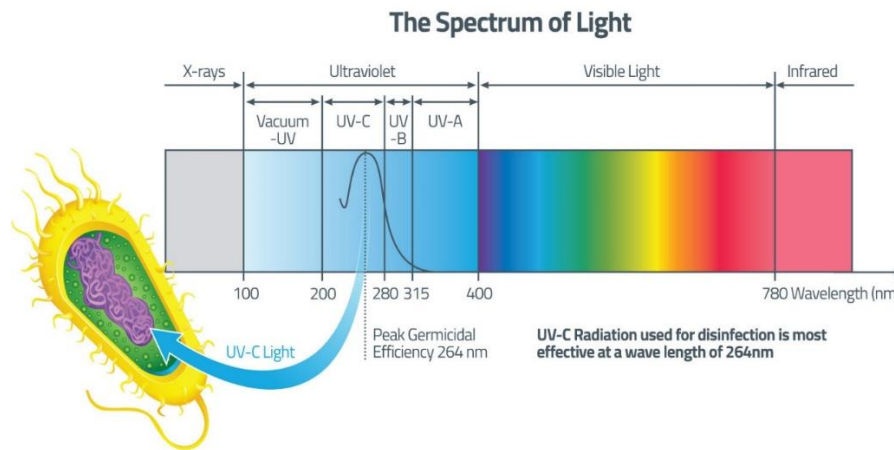


**Fig6: UV-C Radiation For Disinfection**

## **GAMMA IRRADIATION TREATMENT**

Gamma radiation is an ionizing radiation and has been commonly used by maximum containment laboratories to render high-risk group viruses inactive [2]. Gamma irradiation is often the preferred method as it is known to preserve viral morphology and viral protein integrity [3]. Here we sought to determine the radiation dose required for complete inactivation of SARS-CoV-2. The primary mechanism of virus inactivation by ionizing radiation is caused by breakage and crosslinking of genetic material [4-6]. Therefore, we also wanted to see if the gamma irradiation process damaged viral RNA leading to a change in RT-PCR sensitivity. A radiation dose of 1 Mrad was required to completely inactivate 106.5 TCID<sub>50</sub>/ml of SARS-CoV-2 with a calculated D<sub>10</sub> value of 0.16 Mrad. The influence of gamma radiation on PCR sensitivity was inversely related and dose-dependent up to 0.5 Mrad, with no additional reduction thereafter.

### **Materials and Methods**

SARS-CoV-2 (hCoV-19/Canada/ON-VIDO-01/2020, GISAID accession# EPI\_ISL\_425177) was cultured in a high containment laboratory on Vero cells, CCL-81 (ATCC, USA) grown in Minimum Essential Medium (Hyclone, USA) containing 1% fetal bovine serum and 1% L-glutamine. T150 tissue culture flasks with 80-90% confluent cells were infected with SARS-CoV-2 at 1:1000 dilution and incubated at 37°C with 5% CO<sub>2</sub> until 90% cytopathic effect (CPE) became evident (approximately 3 days). The flasks were then harvested and clarified by centrifugation at 6000 x g for 5 minutes. One ml aliquots of the clear supernatant were transferred to 2 ml cryovials tubes (Sarstedt, Germany) and stored at -80°C freezer until irradiation treatment. Gammacell 220 Excel (MDS Nordion Inc. ON, Canada), a self-shielded irradiator with a cobalt-60 source was used for this study. The irradiator's drawer can accommodate a 2L beaker where virus-tubes were placed along with dry ice. The drawer moves down vertically to carry the samples to the sample chamber for irradiation. The irradiator's central absorbed dose rate was 0.114 Mrad/hr when these inactivation experiments were conducted in early April 2020. We used increasing radiation doses of 0, 0.25, 0.5, 1, 2, 3, 4, and 5 Mrads. After irradiation, samples were taken back to the high containment laboratory to determine the viable virus titer in median tissue culture infectious dose (TCID<sub>50</sub>) assay on Vero cells as described previously [7]. Briefly, 100 µL of neat and ten fold dilutions of each treatment was transferred to 96 well plates and incubated as above and read 3 days later; the plates were read for CPE and the TCID<sub>50</sub> was calculated as per Reed and Muench [8]. Negative cultures were confirmed negative by a second passage on Vero cells and monitored for 3 additional days. For the RT-qPCR assay, viral RNA from non-irradiated and irradiated samples was extracted with the Viral RNA Mini kit (Qiagen, Germany), serially diluted from 10<sup>-1</sup> to 10<sup>-7</sup> in 10 mM Tris EDTA and run on a LightCycler 96 (Roche, Germany). The EXPRESS One-Step Superscript RT-qPCR Universal Kit (Invitrogen, USA) was used with primers and probes targeting the envelope (E) and the nucleocapsid (NP) genes [9,10]. Thermal cycling conditions were 50°C for 15 min for reverse transcription, followed by 95°C for 20 seconds and then 40 cycles of 95°C for 3 seconds, 60°C for 30 seconds.

**Irradiation dose required for SARS-COV-2 inactivation**

Complete inactivation of SARS-COV-2 was achieved with 1 Mrad of radiation (Figure 7), which is consistent with previously published data for SARS-CoV-1 [2]. The dose required to reduce the viral titre by one log (D10 value) was determined from the slope of the regression line best fitting the dose curve of the virus from the TCID50 units versus radiation dose (in Mrads). GraphPad Prism (GraphPad Software Inc.) was used for plotting, calculations and statistical analysis. Since a dose of 1 Mrad completely inactivated the virus, data from 2 Mrad and higher were not used for the D10 value calculations. The calculated D10 value for SARS-COV-2 was 0.16 Mrad. **Figure 7.** Inactivation of SARS-COV-2. One ml frozen samples containing 106.5 TCID50/ml of SARS-COV-2 virus were exposed to increasing doses of gamma radiation on dry ice.

**Effect of high irradiation dose on PCR results**

Researchers often expose their high-risk viral samples to many fold higher radiation dose than required for a “complete kill” for added safety. Such high doses of radiation can induce severe damage to the viral RNA leading to unexpected PCR results. Even though our virus sample was completely inactivated upon exposure to 1 Mrad, we subjected our samples to increasing doses of radiation up to 5 Mrad. Viral RNA preparations made from these samples were ten fold serially diluted and tested by RT-qPCR for NP and E genes and plotted against cycle threshold (Cq) (Figure 7).

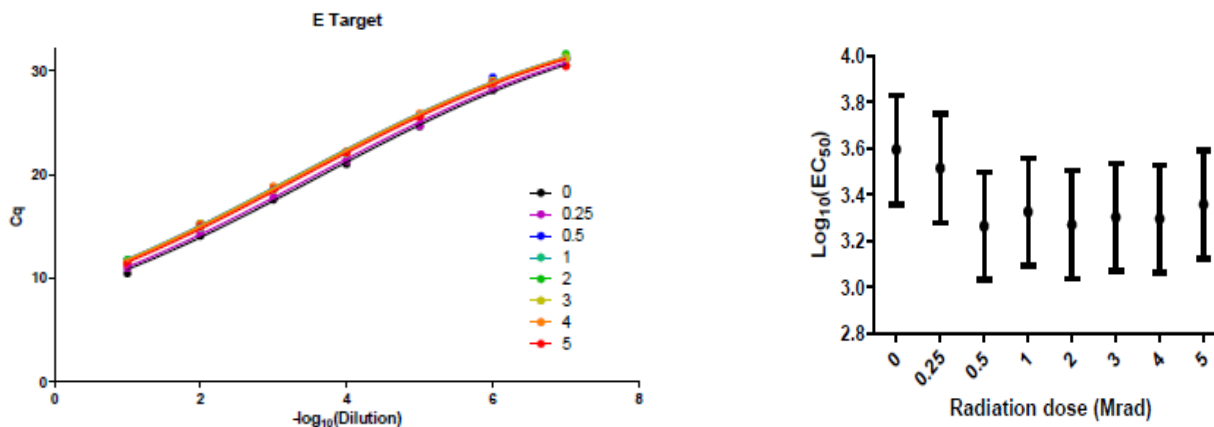


**Fig 7: RT-qPCR for NP and E genes and plotted against cycle threshold (Cq)**

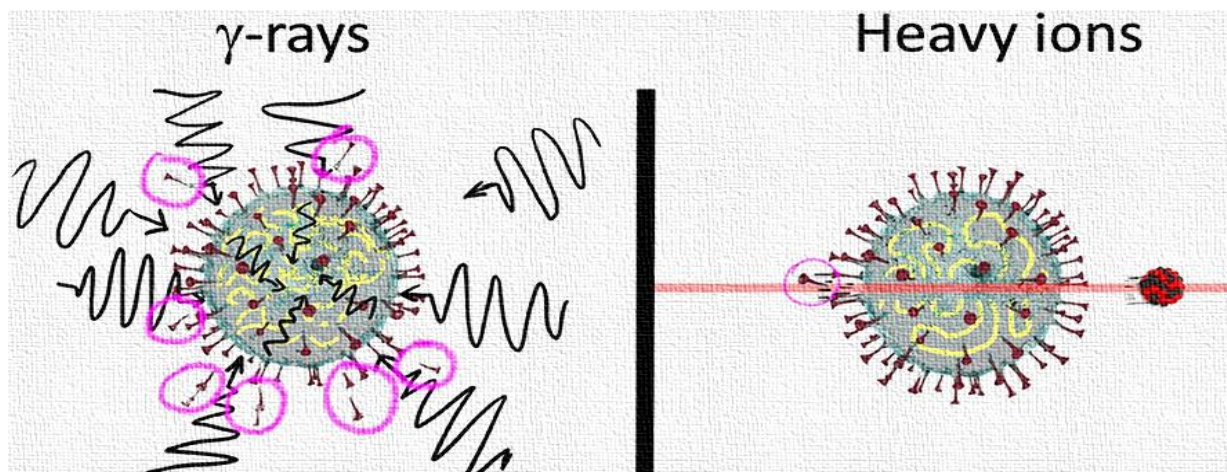


**Figure 8. High- and low-LET radiation for virus inactivation. Schematic representation of the action of sparsely and densely ionizing radiation on SARS-CoV-2. High doses of  $\gamma$ -rays can inactivate the virus, but will damage many membrane proteins, whereas single (or few) heavy ion traversals will produce limited membrane damage while maintaining a high inactivation probability. Sparing of membrane epitopes is essential to elicit the immune response toward vaccine generation.**

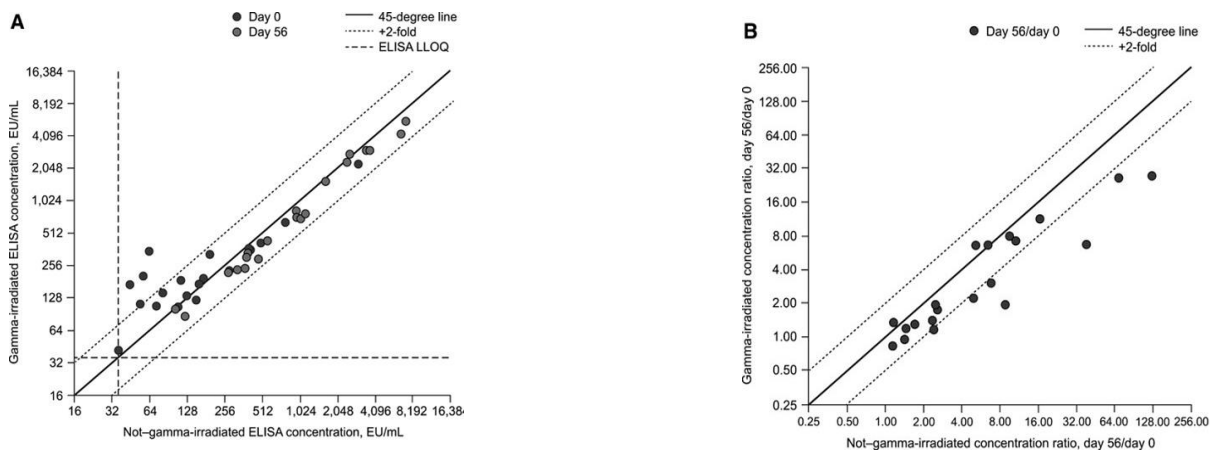


**Fig9: Not-gamma-irradiation ELISA concentration**

**X-RAY IRRADIATION TREATMENT**

Given the importance of inflammatory cascades in the pathogenesis of COVID-19, it is not surprising that LD-RT might find its way into its treatment strategies. Although LD-RT could not reduce the viability of SARS-CoV-2, it may exert its anti-viral responses through modulation of the inflammatory properties of leukocytes, macrophages, fibroblasts, and endothelial cells. The results of Kirkby et al. were, in fact, a confirmation of the application of LD-RT in the treatment of COVID-19. They suggested that administration of 30–100 cGy of radiation to the lungs of a patient with COVID-19 pneumonia could diminish the inflammation, which thereby ameliorates the life-threatening symptoms. It should be mentioned that a single fraction of 30–100 cGy [Fig.10]

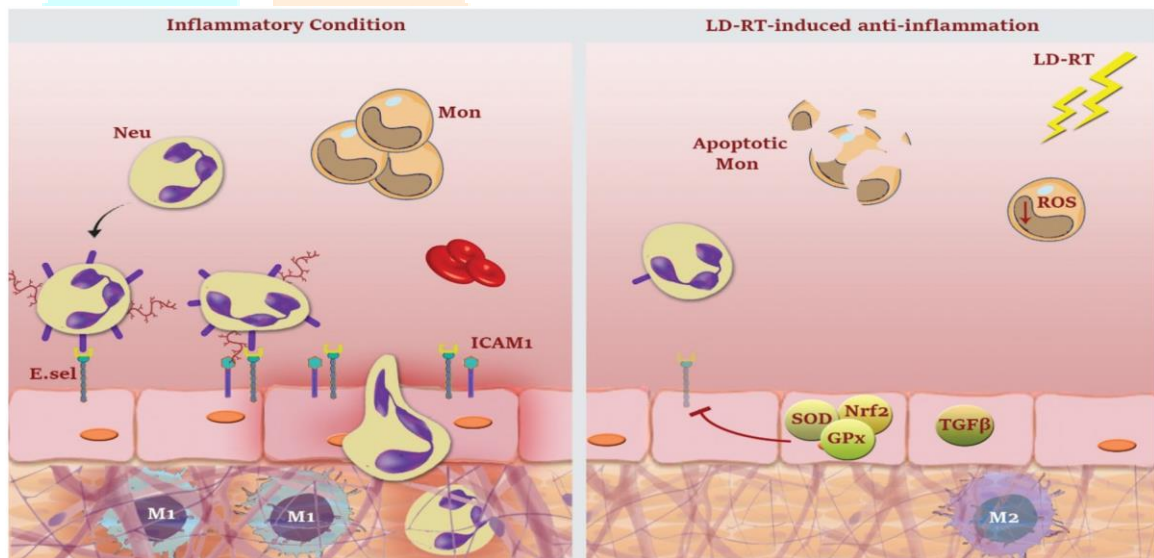


**Figure 10. The mechanisms through which LD-RT induces anti-inflammatory responses.**

In the starting of previous year was coupled with the COVID-19 pandemic, which paralyzed the world’s health care system, economy, and political relations. Every day, a considerable proportion of people, no matter which age group they are, lose their lives due to the lack of appropriate treatment and management protocols. Recently, the application of LD-RT has brought promising advantages for patients, especially for those with unfavorable risk factors. From a theoretical perspective, LD-RT seems to be practical for the treatment of COVID-19 mostly due to its ability to reduce the inflammatory responses through either blocking the secretion of pro-inflammatory cytokines or modulating the activity of monocytes and inflammatory macrophages [6,9,16]. However, due to the restricted data in this area, still, this therapeutic approach could not be recommended for patients. In fact, there are two main concerns about the application of LD-RT in the treatment of COVID-19 patients: (i) the suppression of immune response which may subsequently prolong the elimination of the virus, and (ii) is the risk of cancer development. There are also several unanswered questions about the administration of LD-RT concerning age, clinical condition, right time, the optimum dose, and last but not least, volume and field size. Despite all the indicated concerns, as there are no definite chemical drugs for the treatment of COVID-19-related pneumonia and given the valuable results of LD-RT in ameliorating the acute respiratory syndrome, it seems that conducting researches in this area would be necessary to find an appropriate way to use LD-RT in COVID-19 patients with minimal side effects and the possibility of covid treatment.

**HEAT TREATMENT OF VIRUS**

On incubating 320 µl aliquots of virus in 1.5 ml polypropylene cryotubes using a heating block to achieve three different temperatures (56, 65 and 75 °C) [Fig.7]. After heat treatment, samples were frozen for later analysis by TCID<sub>50</sub> assay using CPE as an endpoint. The viral load of SARS-CoV-2 is 7 × 10<sup>6</sup> per mL on average [14]. To test the capacity of the system to achieve rapid heat inactivation, the researchers used sub-second exposure and found a 6 log 10 or more reduction in viral titer with the oil bath temperature at 115 °C with 1 second residence time. To achieve the same with a lower

exposure time of 0.5 second, the temperature must be raised to 125 °C or more, while if the time is further reduced to 0.25 seconds, the reduction in viral titer is 5 log<sub>10</sub>. At 0.1 second efficient inactivation is not achieved even at 170 °C [17]. Using the residual infectivity, a re-plot showed that the inactivation of the virus required 0.25 seconds at least at an exposure temperature of 85.2 °C. The fastest heat treatment for complete viral inactivation requires 0.5 seconds, with the actual temperature to which the virus is exposed being 83.4 °C

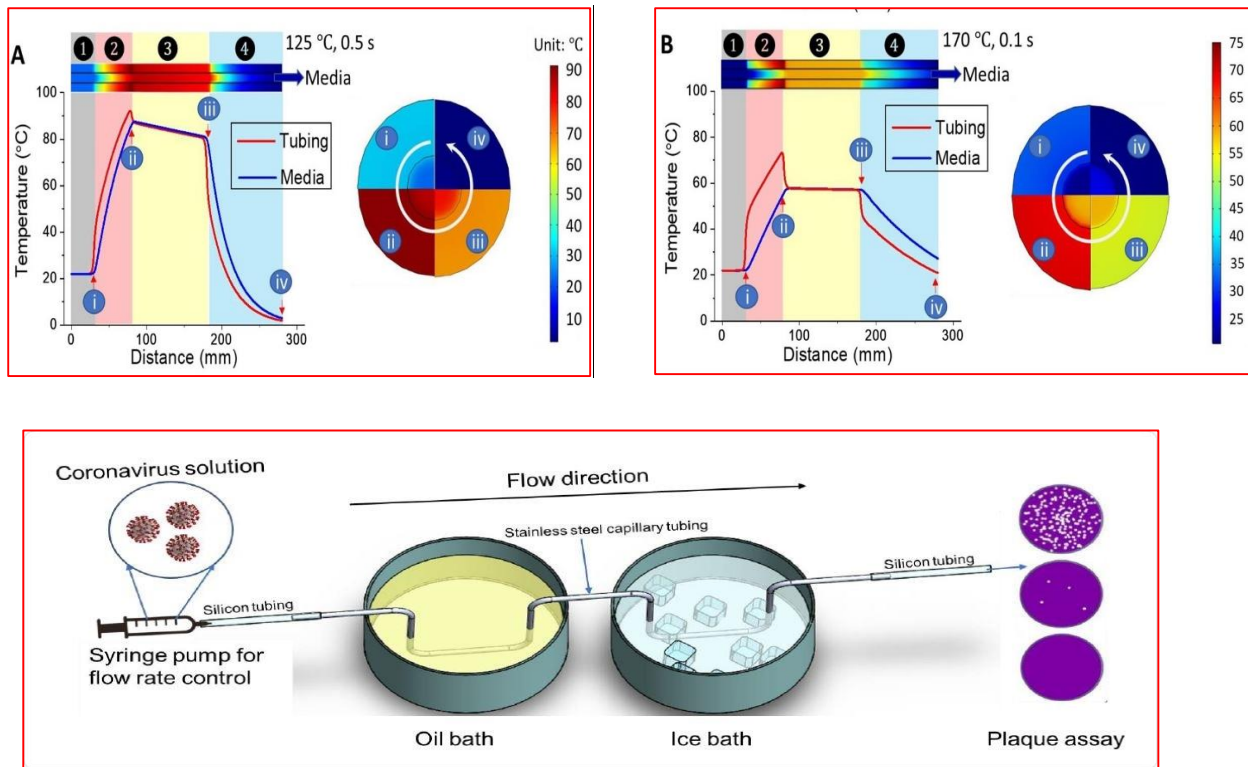


**Fig 11: Heat Treatment of Virus**

### **FORMALDEHYDE AND GLUTARALDEHYDE TREATMENT**

Formaldehyde (37%, Mallinckrodt Baker, Inc., Paris, KY) and glutaraldehyde (8%, Sigma, Saint Louis, MO) were diluted 1:10 and 1:40 in sterile PBS<sup>7</sup>. These diluted aldehydes were added to virus samples to achieve final dilutions of 1:1000 and 1:4000 in 400  $\mu$ l. The final concentrations of formaldehyde were 0.037% (1:1000) and 0.009% (1:4000), and the final concentrations of glutaraldehyde were 0.008% (1:1000) and 0.002% (1:4000). The virus and aldehyde samples were incubated at 4, 25, and 37 °C, for up to 3 days [Fig 11]. The samples were mixed briefly with a vortex on each day. The samples were stored at -70 °C until analysis by TCID<sub>50</sub> assay.

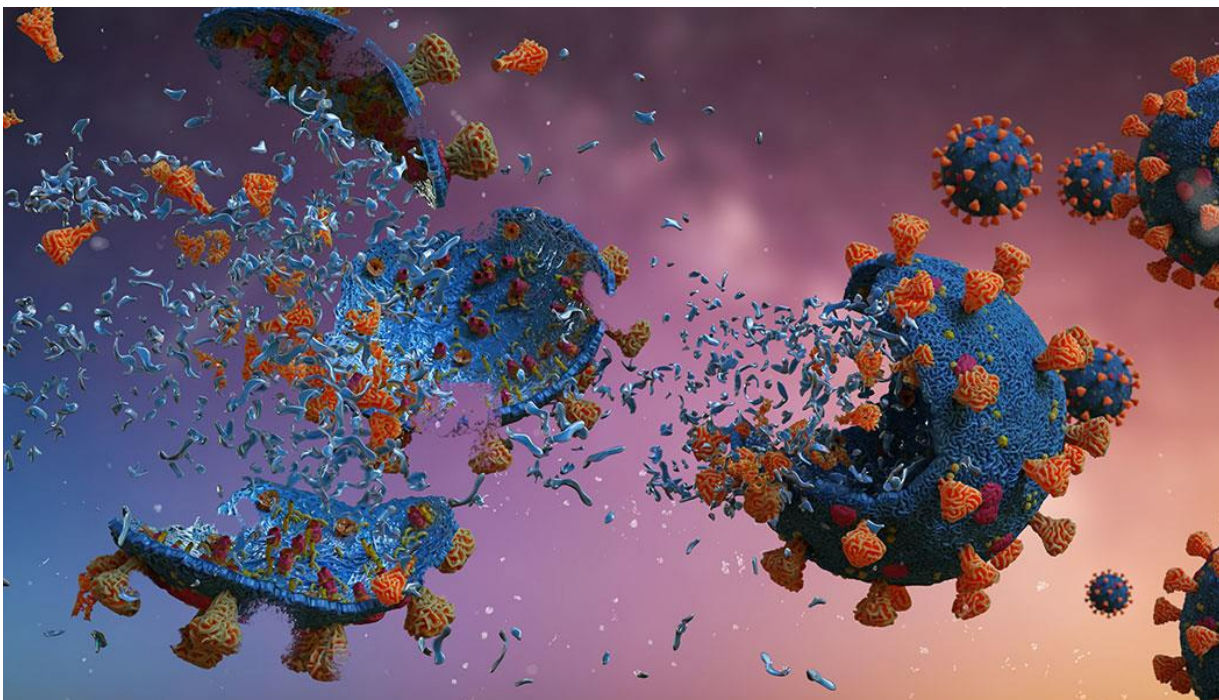


**Fig 12: Formaldehyde and Glutaraldehyde Treatment**

## PH TREATMENT

Severe acute respiratory syndrome (SARS) is a life-threatening disease caused by a novel coronavirus termed SARS-CoV. Due to the severity of this disease, the World Health Organization (WHO) recommends that manipulation of active viral cultures of SARS-CoV be performed in containment laboratories at biosafety level 3 (BSL3). The virus was inactivated by ultraviolet light (UV) at 254 nm, heat treatment of 65 °C or greater, alkaline (pH > 12) or acidic (pH < 3) conditions, formalin and glutaraldehyde treatments[Fig.9]. We describe the kinetics of these efficient viral inactivation methods, which will allow research with SARS-CoV containing materials, that are rendered non-infectious, to be conducted at reduced safety levels. Virus aliquots were adjusted to the desired pH using 5 M and 1 M HCl or 5N and 1N NaOH. Subsequently, they were divided into three aliquots, incubated at the desired temperature (4, 25, and 37 °C), neutralized to a pH 7, and analyzed for viral titer using the TCID<sub>50</sub> assay.

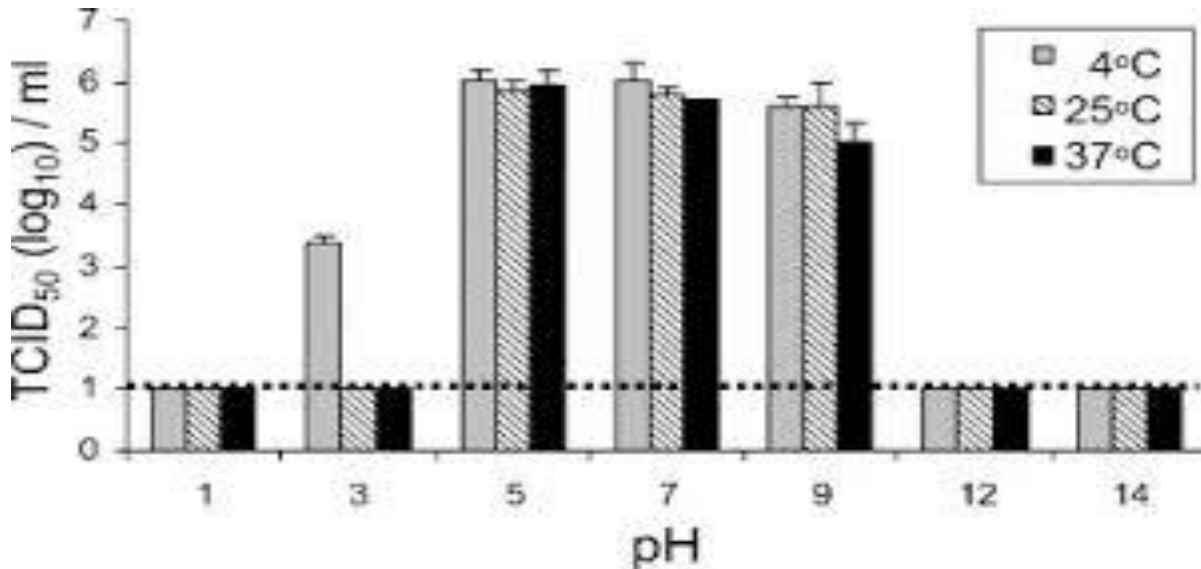


**Fig 12: Variation of TCID<sub>50</sub> with pH at Different Temperature**

## INFECTIVITY OF VIRAL RNA AND DETERGENT-DISRUPTED VIRIONS

Infected Vero cells were prepared by inoculation with 20 µl of virus at a 10<sup>6.37</sup> TCID<sub>50</sub> per ml of SARS-CoV in a final volume of 2 ml in a T25 flask for 1 h at 25 °C. DMEM with supplements was added to the flask and the cells were incubated at 37 °C for 3 days<sup>14</sup>. The monolayer was washed with 1X phosphate buffered saline (PBS), cells were lysed with the addition of 2.5 ml of a phenol and guanidine isothiocyanate solution (TRIzol Reagent, Sigma), and cytoplasmic RNA was isolated according to the manufacturer's specifications. Vero cells were inoculated with 10 µl of purified RNA in 0.5 ml DMEM. After an hour, DMEM with supplements was added. Additionally, Vero cells were transfected with cytoplasmic RNA using DMRIE-C (Invitrogen Life Technologies, Carlsbad, CA) according to the manufacturer's instructions. Cells were incubated at 37 °C, and observed for CPE on days 3 and 4.

To examine the infectivity of detergent-disrupted virions, SARS-CoV infected Vero monolayer cells were washed and dissociated with trypsin/versene, pelleted by centrifugation, and washed with PBS. After centrifugation, the pellet was lysed with sodium dodecyl sulfate/nonidet P-40 (SDS/NP-40; 0.1% SDS, 0.1% NP-40, in 0.1x PBS; Sigma), frozen at -70 °C, thawed, and clarified by centrifugation. The supernatant was used to infect Vero cell monolayers in 6-well plates, such that the final concentration of SDS was 0.002 or 0.018%. Three and four days following the inoculation, cells were observed for evidence of CPE.

## **RESULTS**

### EFFECT OF RADIATION ON THE INFECTIVITY OF SARS-COV

UV light is divided into three classifications: UVA (320–400 nm), UVB (280–320 nm), and UVC (200–280 nm). UVC is absorbed by RNA and DNA bases, and can cause the photochemical fusion of two adjacent pyrimidines into covalently linked dimers, which then become non-pairing bases. UVB can cause the induction of pyrimidine dimers, but 20–100-fold less efficiently than UVC. UVA is weakly absorbed by DNA and RNA, and is much less effective than UVC and UVB in inducing pyrimidine dimers, but may cause additional genetic damage through the production of reactive oxygen species, which cause oxidization of bases and strand breaks.

To examine the inactivation potential of UVA and UVC, virus stocks were placed in 24-well tissue culture plates and exposed to UV irradiation on ice for varying amounts of time, as indicated in Fig.13A. Exposure of virus to UVC light resulted in partial inactivation at 1 min with increasing efficiency up to 6 min (Fig.13A), resulting in a 400-fold decrease in infectious virus. No additional inactivation was observed from 6 to 10 min. After 15 min the virus was completely inactivated to the limit of detection of the assay, which is ≤1.0 TCID<sub>50</sub> (log<sub>10</sub>) per ml. In contrast, UVA exposure demonstrated no significant effects on virus inactivation over a 15 min period. Our data show that UVC light inactivated the SARS virus at a distance of 3 cm for 15 min.



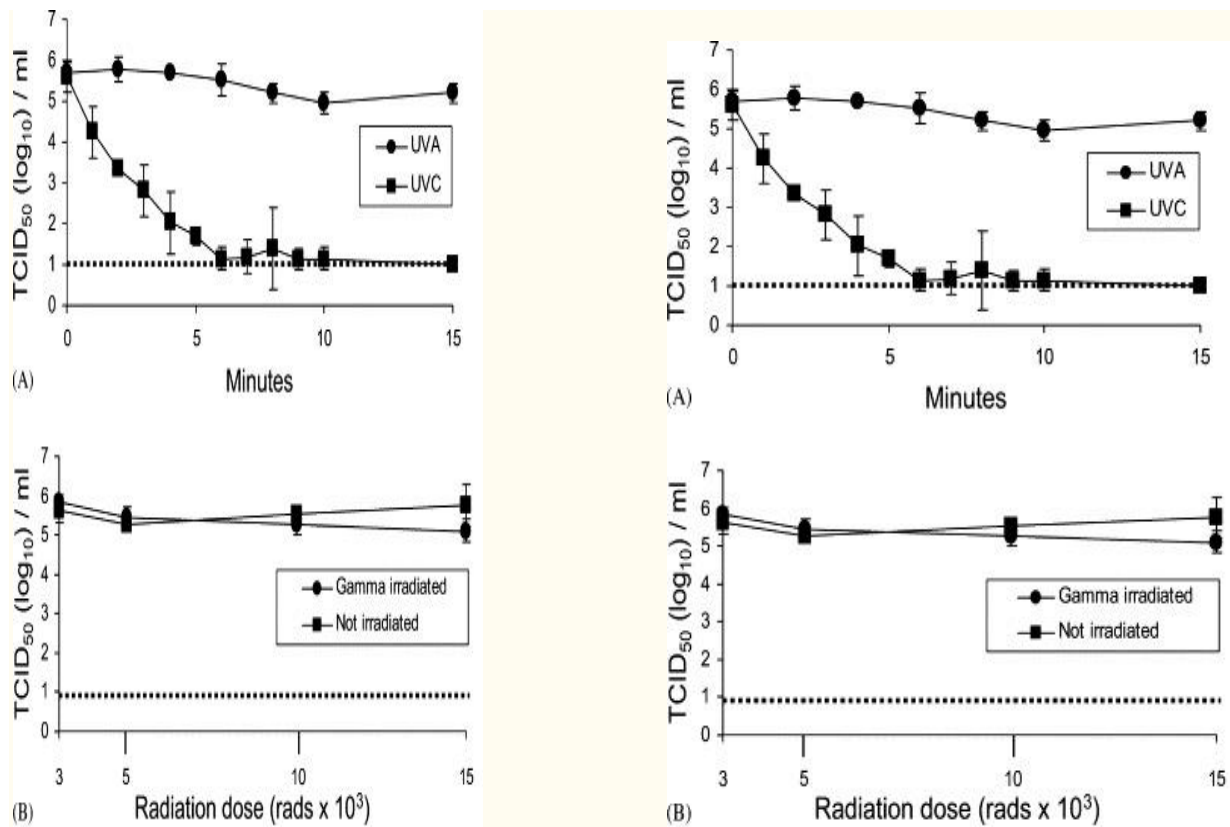


**Fig. 13:** Effect of radiation on the infectivity of SARS-CoV. (A) UV irradiation. The UV lamp was placed 3 cm above the bottom of 24-well plates containing 2 ml virus aliquots. Samples were removed at each time point, frozen, and titrated in Vero E6 cells. The results shown are representative of three independent experiments. (B) Gamma irradiation. Virus aliquots (400  $\mu$ l) were placed in cryovials on dry ice and exposed to the indicated dose of gamma irradiation. Control samples were treated identically, without radiation exposure. Samples were titrated in Vero E6 cells in triplicate. The dotted line denotes the limit of detection of the assay.

A standard procedure to inactivate viruses during the manufacture of biological products is gamma irradiation. To investigate the effect of gamma irradiation on SARS-CoV, we subjected 400  $\mu$ l of SARS-CoV to gamma radiation (3000, 5000, 10,000, and 15,000 rad) from a  $^{60}\text{Co}$  source, while control samples were protected from exposure. No effect on viral infectivity was observed within this range of gamma irradiation exposure (Fig.10B).

### **EFFECT OF HEAT TREATMENT ON THE INFECTIVITY OF SARS-COV**

Heat can inactivate viruses by denaturing the secondary structures of proteins, and thereby may alter the conformation of virion proteins involved in attachment and replication within a host cell. To test the ability of heat to inactivate the SARS-CoV, we incubated virus in 1.5 ml polypropylene cryotubes at three temperatures (56, 65 and 75  $^{\circ}\text{C}$ ) for increasing periods of time. We found that at 56  $^{\circ}\text{C}$  most of the virus was inactivated after 20 min (Fig.14A). However, the virus remained infectious at a level close to the limit of detection for the assay, for at least 60 min, suggesting that some virus particles were stable at 56  $^{\circ}\text{C}$  (Fig.6A and C). At 65  $^{\circ}\text{C}$ , most of the virus was inactivated if incubated for longer than 4 min (Fig.14B). Again, some infectious virus could still be detected close to the limit of detection for the assay, after 20 min at 65  $^{\circ}\text{C}$ . While virus was incompletely inactivated at 56 and 65  $^{\circ}\text{C}$  even at 60 min, it was completely inactivated at 75  $^{\circ}\text{C}$  in 45 min (Fig.11C). Surprisingly, at both 56 and 65  $^{\circ}\text{C}$  the virus was inactivated at early time points but at 60 min a small amount of virus was detected. One possible explanation for this result may be the presence and subsequent dissociation of aggregates. Taken together, these results suggest that viral inactivation by pasteurization may be very effective.

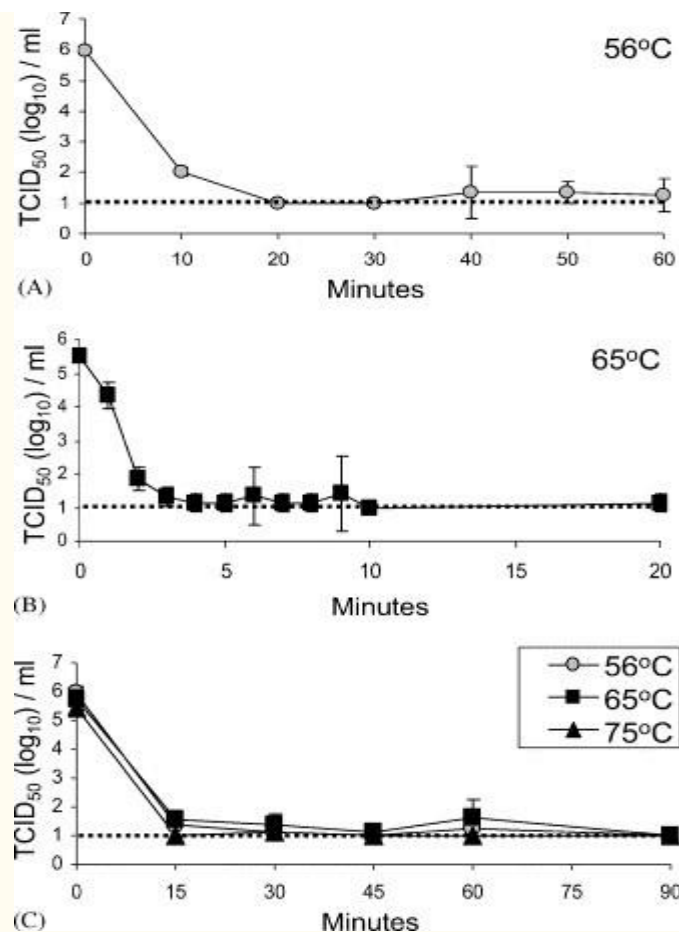


**Fig. 14:**Effect of heat treatment on the infectivity of SARS-CoV. Virus aliquots (400  $\mu$ l) were incubated at (A, C) 56 °C, (B, C) 65 °C and (C) 75 °C. Samples were removed at the designated time, frozen, and titrated in Vero E6 cells in triplicate. The dotted line denotes the limit of detection of the assay.

Formalin (dilute formaldehyde) has been used for a number of years to inactivate virus for use in vaccine products, such as the widely used and very effective polio vaccine. Other attempts at using formalin inactivation for generation of vaccines for respiratory syncytial virus and measles virus were not useful, as they induced an aberrant immune response resulting from formalin-induced perturbations of the viruses. Formalin inactivation occurs when nonprotonated amino groups of amino acids, such as lysine, combine with formaldehyde to form hydroxymethylamine. The hydroxymethylamine combines with the amino, amide, guanidyl, phenolic, or imidazole group of amino acids to create inter- or intramolecular methylene crosslinks. Frankel-Conrat observed the absorption spectra of several plant viruses and determined that formalin also binds in a reversible manner to RNA, blocking reading of the genome by RNA polymerase. Glutaraldehyde can also be used to inactivate virus and is used as a disinfecting agent of medical instruments, such as endoscopes and as a fixative for electron microscopy.

On examining formalin and glutaraldehyde inactivation of the SARS-CoV by incubating virus samples with formalin or glutaraldehyde at two different dilutions (1:1000 and 1:4000). Each of the diluted aldehydes was incubated with virus at 4, 25 or 37 °C. Both of the aldehydes exhibited temperature dependence in their ability to inactivate virus. Neither formalin nor glutaraldehyde, at a 1:4000 dilution, was able to completely inactivate virus at 4 °C, even after exposure for 3 days. At 25 and 37 °C, formalin inactivated most of the virus, close to the limit of detection of the assay, after 1 day, yet some virus still remained infectious on day 3. However, glutaraldehyde completely inactivated the virus by day 2 at 25 °C and by day 1 at 37 °C. This suggests that both formalin and glutaraldehyde inactivation of SARS virus may be efficient methods of inactivation, if proper conditions are met.

## References

1. Dietz L, Horve PF, Coil DA, et al. 2019 novel coronavirus (COVID-19) pandemic: built environment considerations to reduce transmission. *mSystems*. 2020; **5**(2): e00245.
2. Jin Y-H, Cai L, Cheng Z-S, et al. A rapid advice guideline for the diagnosis and treatment of 2019 novel coronavirus (2019-nCoV) infected pneumonia (standard version). *Mil Med Res*. 2020; **7**: 4.
3. Manganello K. Xenex LightStrike robot destroys SARS-CoV-2 (coronavirus) in 2 minutes [Internet]. San Antonio: Xenex; 2020 Apr 30 [cited 2020 May 15].
4. Moore SK. Flight of the GermFalcon: how a potential coronavirus-killing airplane sterilizer was born [Internet]. New York: IEEE Spectrum; 2020 Mar 9 [cited 2020 May 15].
5. Mackenzie D. Reuse of N95 masks. *Engineering* 2020;6 (6):593–6.
6. Bolton JR. UV FAQs [Internet]. Chevy Chase: International Ultraviolet Association; [cited 2020 May 15].
7. Malayeri AH, Mohseni M, Cairns B, Bolton JR. Fluence (UV dose) required to achieve incremental log inactivation of bacteria, protozoa, viruses, and algae [Internet]. Chevy Chase: IUVA News; [cited 2020 May 15].
8. Ackerman E. Autonomous robots are helping kill coronavirus in hospitals; [Internet]. New York: IEEE Spectrum; 2020 Mar 11 .
9. Emmanuel T, Lybæk D, Johansen C, Iversen L. Effect of dead sea climatotherapy on psoriasis. A prospective cohort study. *Front Med (Lausanne)*. 2020; **7**: 83.
10. Buonanno M., Ponnaiya B., Welch D., Stanislauskas M., Randers-Pehrson G., Smilenov L. Germicidal efficacy and mammalian skin safety of 222-nm UV light. *Radiat Res*. 2017;187:493–501.
11. Welch D., Buonanno M., Grilj V., Shuryak I., Crickmore C., Bigelow A.W. Far-UVC light: a new tool to control the spread of airborne-mediated microbial diseases. *Sci Rep*. 2018;8:2752.
12. Lindblad M., Tano E., Lindahl C., Huss F. Ultraviolet-C decontamination of a hospital room: amount of UV light needed. *Burns*. 2019;46(4):842–849.
13. Edridge A.W., Kaczorowska J.M., Hoste A.C., Bakker M., Klein M., Jebbink M.F., Matser A., Kinsella C., Rueda P., Prins M., et al. Coronavirus protective immunity is short-lasting. *medRxiv*. 2020 doi: 10.1101/2020.05.11.20086439.
14. Lan L., Xu D., Ye G., Xia C., Wang S., Li Y., Xu H. Positive RT-PCR Test Results in Patients Recovered From COVID-19. *JAMA*. 2020 doi: 10.1001/jama.2020.2783.
15. Tillett R.L., Sevinsky J.R., Hartley P.D., Kerwin H., Crawford N., Gorzalski A., Laverdure C., Verma S.C., Rossetto C.C., Jackson D., et al. Genomic evidence for reinfection with SARS-CoV-2: A case study. *Lancet Infect. Dis*. 2020 doi: 10.1016/S1473-3099(20)30764-7.
16. Long Q.X., Tang X.J., Shi Q.L., Li Q., Deng H.J., Yuan J., Hu J.L., Xu W., Zhang Y., Lv F.J., et al. Clinical and immunological assessment of asymptomatic SARS-CoV-2 infections. *Nat. Med*. 2020 doi: 10.1038/s41591-020-0965-6.
17. Grifoni A., Weiskopf D., Ramirez S.I., Mateus J., Dan J.M., Moderbacher C.R., Rawlings S.A., Sutherland A., Premkumar L., Jadi R.S., et al. Targets of T Cell Responses to SARS-CoV-2 Coronavirus in Humans with COVID-19 Disease and Unexposed Individuals. *Cell*. 2020;181:1489.e1415–1501.e1415. doi: 10.1016/j.cell.2020.05.015.
18. Le Bert N., Tan A.T., Kunasegaran K., Tham C.Y.L., Hafezi M., Chia A., Chng M.H.Y., Lin M., Tan N., Linster M., et al. SARS-CoV-2-specific T cell immunity in cases of COVID-19 and SARS, and uninfected controls. *Nature*. 2020 doi: 10.1038/s41586-020-2550-z.
19. He R., Lu Z., Zhang L., Fan T., Xiong R., Shen X., Feng H., Meng H., Lin W., Jiang W., et al. The clinical course and its correlated immune status in COVID-19 pneumonia. *J. Clin. Virol*. 2020;127:104361. doi: 10.1016/j.jcv.2020.104361.
20. Liu Z., Long W., Tu M., Chen S., Huang Y., Wang S., Zhou W., Chen D., Zhou L., Wang M., et al. Lymphocyte subset (CD4+, CD8+) counts reflect the severity of infection and predict the clinical outcomes in patients with COVID-19. *J. Infect*. 2020;81:318–356. doi: 10.1016/j.jinf.2020.03.054.